ACS APPLIED MATERIALS & INTERFACES

Research Article

www.acsami.org

A Facile One-Pot Method to Synthesize a Polypyrrole/Hemin Nanocomposite and Its Application in Biosensor, Dye Removal, and Photothermal Therapy

Peng Hu,[†,‡] Lei Han,[†,‡] and Shaojun Dong*[,†,‡]

[†]State Key Laboratory of Electroanalytical Chemistry, Changchun Institute of Applied Chemistry, Chinese Academy of Science, Changchun, Jilin, 130022, China

[‡]University of Chinese Academy of Sciences, Beijing, 100049, China

Supporting Information

ABSTRACT: In this work, we introduced a facile method for the construction of a polypyrrole/hemin (PPy/hemin) nanocomposite via one-pot chemical oxidative polymerization. In this process, a hemin molecule serving as a dopant was entrapped in the PPy nanocomposite during chemical oxidative polymerization. Scanning electron microscopy (SEM), transmission electron microscopy (TEM), Fourier transform infrared spectroscopy (FTIR), and UV−visible spectroscopy results demonstrated that the PPy/hemin nanocomposite was successfully synthesized. The as-prepared nanocomposite exhibited intrinsic peroxidase-like catalytic activities, strong adsorption properties, and an excellent near-infrared (NIR) light-induced thermal effect. We utilized the nanomaterials to catalyze the oxidation of a peroxidase substrate 3,3,5,5-tetramethylbenzidine by H_2O_2 to the oxidized colored product which provided a colorimetric detection of glucose. As low as 50 μM glucose could be detected with a linear range from 0.05 to 8 mM. Moreover, the obtained nanocomposite also showed excellent removal efficiency for methyl orange and rhodamine B and a photothermal effect, which implied a promising application as the pollutant adsorbent and photothermal agent. The unique nature of the PPy/hemin nanocomposite makes it very promising for the fabrication of inexpensive, high-performance bioelectronic devices in the future.

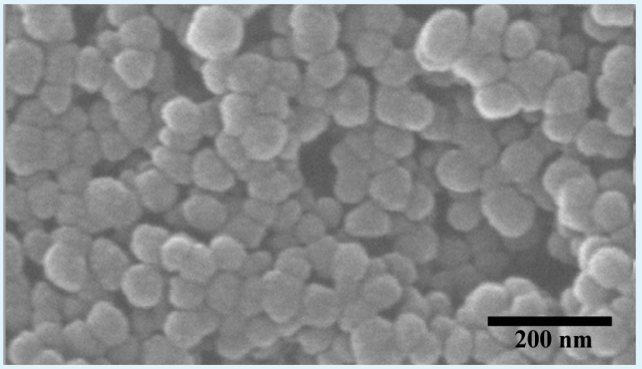

KEYWORDS: *polypyrrole, hemin, nanocomposite, biosensor, dye removal, photothermal effect*

1. INTRODUCTION

Since the 1960s, conducting polymers (CPs) have been the subject of numerous studies because of their potential applications in optical and electrical fields.[1−6] Among the CP family, polypyrrole (PPy) is regarded as one of the most prominent and attractive materials due to its unique properties, such as low cost, easy preparation, tunable conductivity, air stable, and biocompatibility.[7−11] Owing to these advantages, great efforts have been made to develop PPy-based nanomaterials and explore their applications in biosensors, electronics and optoelectronics, energy storage, enzyme immobilization, and so on. For instance, Dong et al. fabricated an electrochemical chloride ion sensor by electrodepositing PPy film on chromatography paper.[12] The film acted as a selective sensing interface and achieved sensitive, rapid, and miniature detection. Dong and co-workers constructed graphene oxide/PPy nanocomposite film via one-step co-electrodeposition.[13] The obtained film exhibited good electrochemical properties and cycling performance, which should be very promising for the fabrication of inexpensive, high-performance electrochemical supercapacitors. De Paoli's group designed a functional PPy coating which doped indigo carmine dye into PPy/dodecylsulfate film.[14] The film could switch between the conducting and insulating forms and hold promise for applications in electrochromic devices. However, previous investigations of PPy have been predominantly focused on the properties of electrical conductivity and electroactivity in electrochemical applications.[2,3,6,9,11−13] The special nature of the materials in the liquid phase has not attached much importance due to the drawbacks of being mechanically weak and having poor dispersibility.[15] In this case, it has been a subject of intensive interest to synthesize PPy-based nanomaterials in colloidal form to improve the processability of the intractable material.

Peroxidases are a large family of enzymes that typically catalyze the oxidation of inorganic and organic substrates at the expense of an assortment of peroxides.[16] For many of these enzymes, the optimal substrate is hydrogen peroxide, but others

Received: October 16, 2013
Accepted: December 5, 2013
Published: December 5, 2013

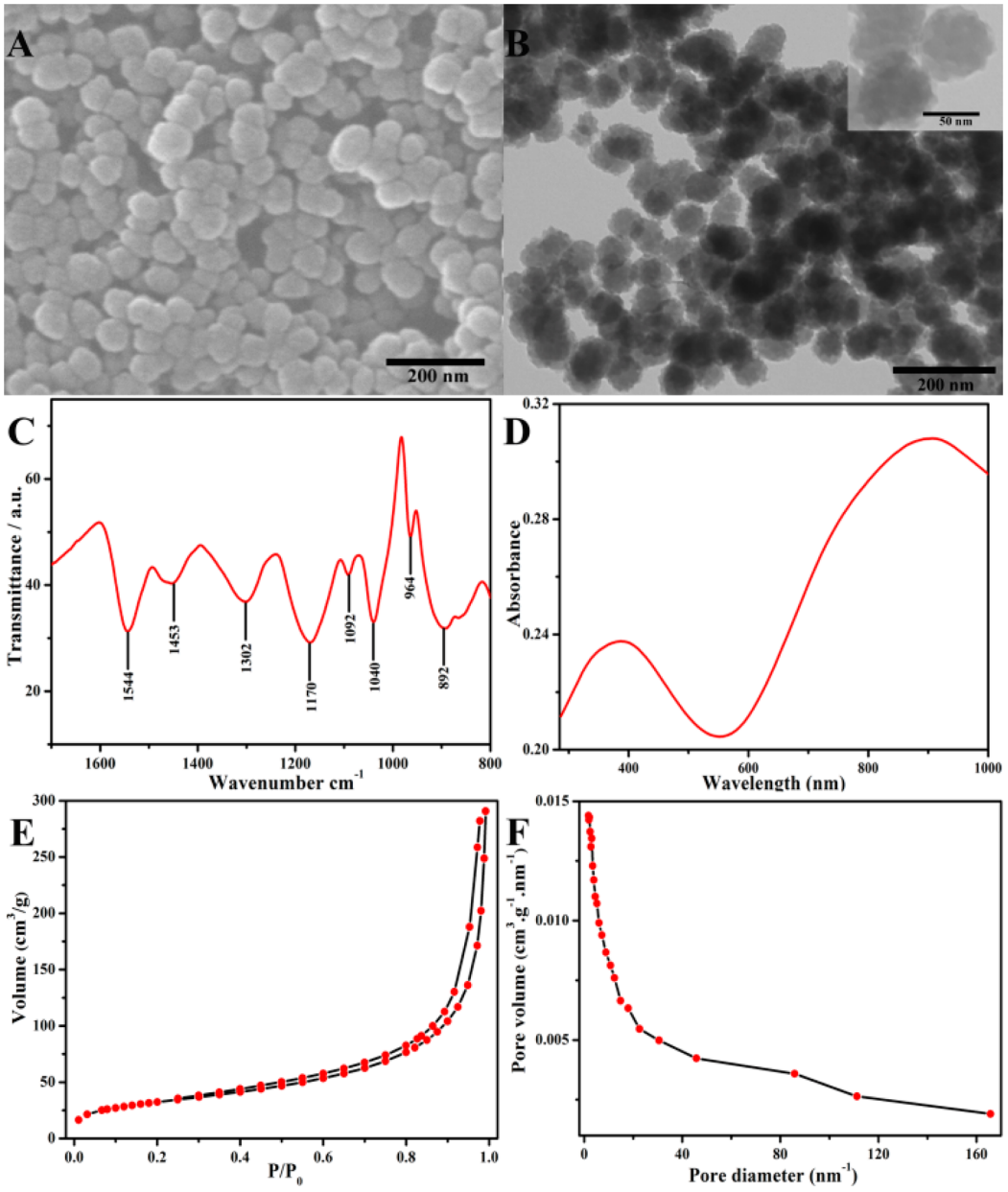

Figure 1. (A) SEM and (B) TEM images of the as-synthesized PPy/hemin nanocomposite. (C) FTIR and (D) UV−vis spectra of the nanocomposite. (E) Nitrogen adsorption−desorption isotherms and (F) pore size distribution of the as-obtained nanocomposite.

are more active with organic hydroperoxides. Until now, numerous applications of peroxidases have been found in fields such as biosensors, immunoassays, cell growth, and pollutant removal.[17−31] Though these reports have been demonstrated as useful tools for bioanalysis, molecular diagnostics, and environmental chemistry, the deficiencies such as instability, high cost of enzymes, or critical operating situation may pose limitations in their applications. Recently, artificial enzymes, which could mimic the structures and functions of the natural enzymes, have emerged as a promising alternative due to their highly stable and low-cost characteristics.[32−36] Some hemin-based composites are such alternatives that exhibit unexpected enzyme-like activity and have been employed in various fields.[37−40] Our group proposed for the first time a simple wet-chemical strategy for synthesizing hemin-graphene hybrid nanosheets (H-GNs).[41] Taking advantage of the intrinsic peroxidase-like activity of the H-GNs, a label-free colorimetric detection system for single-nucleotide polymorphisms (SNPs) in disease-associated DNA was developed. Additionally, G-quadruplex DNAzyme also exhibits superior peroxidase-like activity. Wang et al. developed a novel bifunctional colorimetric oligonucleotide probe for DNA and thrombin detection by coupling G-quadruplex DNAzyme with a molecular beacon.[42] They also built a series of label-free colorimetric logic gates based on the formation and dissociation of G-quadruplex DNAzyme, which acted as logic gates that were necessary for the development of DNA computers with high speed and outstanding data storage capacity.[43] However, these hemin-based artificial enzymes may still suffer from the limitations of instability, deliberately designed nucleic acid sequences, or tedious synthesis steps, increasing the difficulty in applying it for large-scale assays and molecular diagnostics. Therefore, it is still a central challenge to develop artificial enzymes that are stable, easily prepared, and cost-efficient.

dx.doi.org/10.1021/am404539j | ACS Appl. Mater. Interfaces 2014, 6, 500−506

In the present study, a novel PPy/hemin nanocomposite was successfully prepared by combining pyrrole monomer with hemin molecule via chemical oxidative polymerization. Pluronic123 was used as a template kit and steric stabilizer. The obtained nanocomposite was easily dispersed in aqueous solution and exhibited intrinsic peroxidase-like catalytic activities, strong adsorption properties, and excellent near-infrared (NIR) light-induced thermal effects. Its applications in glucose biosensors, pollutant removal, and photothermal effect were simultaneously investigated in the following experiments. It is noted that PPy/hemin as enzymatic mimics in an aqueous colloidal solution, to our knowledge, has not been explored to date. Moreover, taking advantage of high stability, efficiency, and controlled preparation at low cost, the PPy/hemin has potential applications in clinical diagnosis and environmental protection.

2. MATERIALS AND METHODS

2.1. Materials. Pluronic123, pyrrole, and 3,3,5,5-tetramethylbenzidine (TMB) were purchased from Sigma-Aldrich. Glucose oxidase (GOD) (E.C.1.1.3.4, 100 U mg^{-1}, from *Aspergillus niger*) and other chemicals were reagent grade and were used without further purification. All aqueous solutions were prepared with ultra-pure water (>18 MΩ) from a Milli-Q Plus system (Millipore).

2.2. Apparatus. UV−vis absorbance spectra were carried out on a Cary 500 Scan UV−visible spectrophotometer (Varian, USA). Transmission electron microscopy (TEM) measurements were made on a HITACHI H-8100 EM with an accelerating voltage of 200 kV. The scanning electron microscope (SEM) images were taken with an XL30 field-emission SEM at an accelerating voltage of 15 kV. Infrared spectra were obtained on a VERTEX 70 Fourier transform infrared (FTIR) spectrometer (Bruker). Photothermal data were recorded by 808 nm NIR laser (Hi-Tech Optoelectronics Co., Ltd. Beijing, China).

2.3. Synthesis of PPy/Hemin Nanocomposite. Pluronic123 (0.4 g) was first dissolved in 50 mL of H_2O by continuous stirring to form a homogeneous and transparent solution. Pyrrole monomer (270 μL) and hemin (1 μmol) were then added dropwise to the surfactant solution, respectively. Finally, $FeCl_3$ (4.32 g) dissolved in 7 mL of H_2O was added to the surfactant/pyrrole solution slowly under vigorous stirring. The reaction maintained at room temperature for 24 h, and the products were washed several times with ethanol and dried at 60 °C.

2.4. Glucose Determination. In a typical glucose assay, an appropriate concentration of glucose (10 μL) was added to a centrifugal tube containing PPy/hemin (2 mg/mL, 10 μL), TMB (10 mM, 10 μL), GOD (1 mg/mL, 10 μL), and NaAc−HAc buffer (0.2 M, 760 μL, pH 4.0). The mixture was incubated at 37 °C for 20 min. Then, H_2SO_4 (2.0 M, 200 μL) was added into the solution to stop the reaction. The absorption spectrum was collected on an UV−visible spectrophotometer, and the photos were taken immediately after stopping the reaction.

2.5. Dye Adsorption. A serial volume of PPy/hemin (1 mg/mL) was added to methyl orange (MO) or rhodamine B (RB) (10 mg/mL, 1 mL) aqueous solution, respectively. The mixtures were maintained for a certain time and separated by centrifuge. The supernatants were recorded on an UV−visible spectrophotometer.

3. RESULTS AND DISCUSSION

3.1. Materials Characterization. We first investigated the morphology of the as-prepared PPy/hemin by SEM and TEM. As can be seen from Figure 1A, the SEM image shows that the PPy/hemin possesses an approximate spherical morphology with an average diameter of about 60 nm. The monodisperse nanostructure was further confirmed by TEM (Figure 1B) imaging. The FTIR spectrum (Figure 1C) featured several characteristic bands.[44−46] The bands at 892, 1040, and 964 cm^{-1} are due to C−H in- and out-of-plane and C−C in-plane vibration, respectively. The band at 1170 cm^{-1} is caused by the vibration of the aromatic pyrrole ring. The peaks at 1544 and 1453 cm^{-1} are attributed to the C−C, C−N, and N−H stretching vibrations in the pyrrole ring.[13] The UV−vis−NIR spectrum of PPy/hemin (Figure 1D) revealed a strong and broad bipolaron absorption in the region from 700 to 1000 nm, which agrees well with the previous report.[46] The surface area and porosity of the final product were determined from N_2 physisorption isotherms (Figure 1E). The surface area as estimated from a Brunauer− Emmett−Teller (BET) plot is 115.17 m^2 g^{-1}, and the average pore width (Figure 1F) is 9.2 nm.

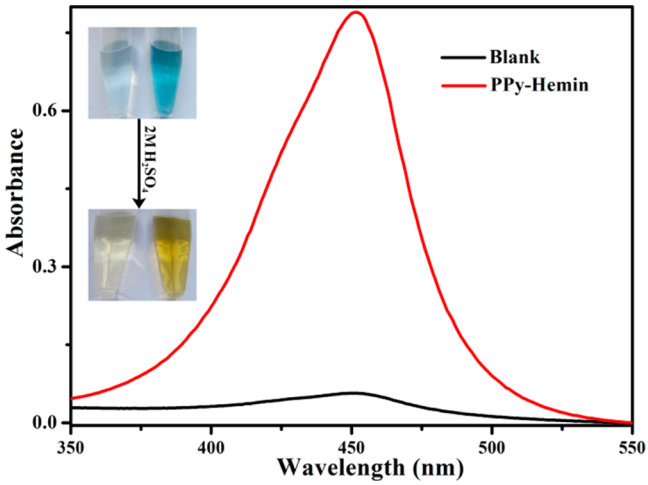

Figure 2. The absorption spectra and digital photos of colorimetric reaction of TMB and H_2O_2 in NaAc buffer solutions (0.2 M, pH 4.0) without and with PPy/hemin nanocomposite.

3.2. Peroxidase-Like Activity of PPy/Hemin. Many peroxidases are heme proteins and utilize hemin as their cofactor.[47−49] Previous studies hypothesized that the hydrophobic protein microenvironment of the hemin moiety in peroxidases exerted a specific and multifaceted enhancing role on the intrinsic peroxidatic property of the hemin.[16,50] On the basis of this speculation, we synthesized hemin doped PPy nanoparticles. In this process, hemin molecule that served as a dopant was entrapped in the PPy nanocomposite during chemical oxidative polymerization and the water-insoluble PPy could provide a hydrophobic external environment for it. Therefore, hemin molecule could serve as a catalytic center and exhibit intrinsic peroxidase-like activity. To confirm the feasibility of this conjecture, we performed the colorimetric experiment using PPy/hemin as an activator. As expected, the nanocomposite could effectively catalyze the H_2O_2-mediated oxidation of TMB to generate the typical blue color reaction under experimental conditions. (The color changed to yellow after 2.0 M H_2SO_4 was added into the solution to stop the reaction, shown in the inset of Figure 2). Conversely, the TMB−H_2O_2 system without PPy/hemin showed slight color variation and the system with PPy or hemin demonstrated similar results (as shown in Figure S1, Supporting Information). Additionally, PPy/hemin couldn't catalyze TMB to produce the color change in the absence of H_2O_2. We also repeated the experiments using *O*-phenylenediamine as substrates instead of TMB. Figure S2 (Supporting Information) shows that PPy/hemin not only catalyzed oxidation of TMB,

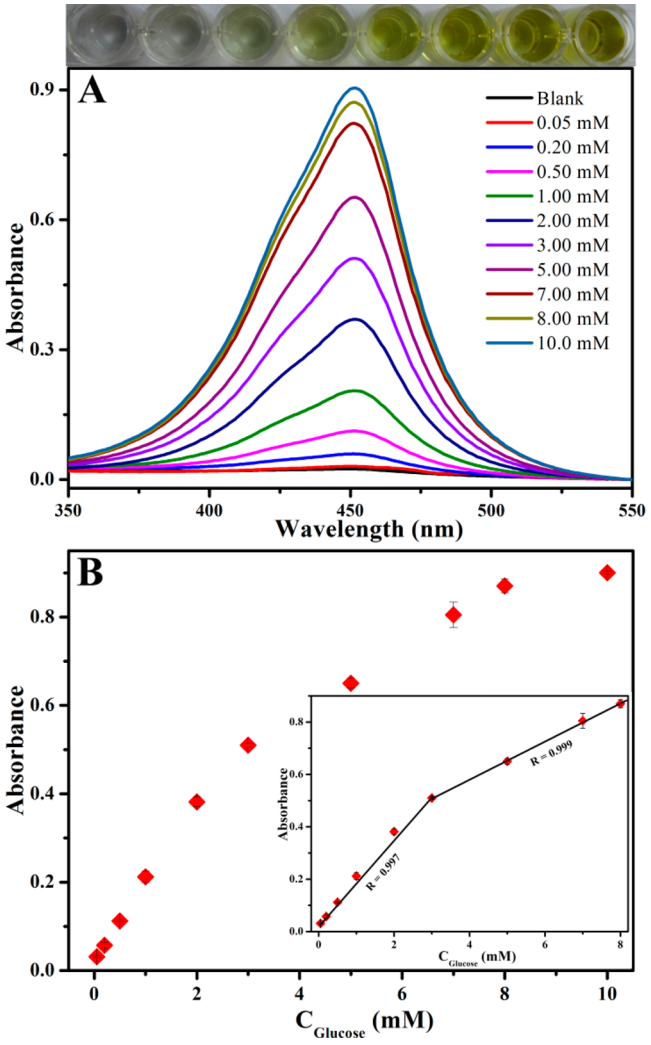

Figure 3. Colorimetric analysis for glucose: (A) UV−vis absorption of different concentrations of glucose ranging from 0 to 10.00 mM. (B) Dose dependency curve of absorption intensity versus the target concentration. The inset shows the calibration curve for target molecule concentration ranging from 0.05 to 8.00 mM. The error bars are the standard deviation (SD) across three repetitive experiments. The photograph above part A shows the color change of the detecting system under different glucose concentrations.

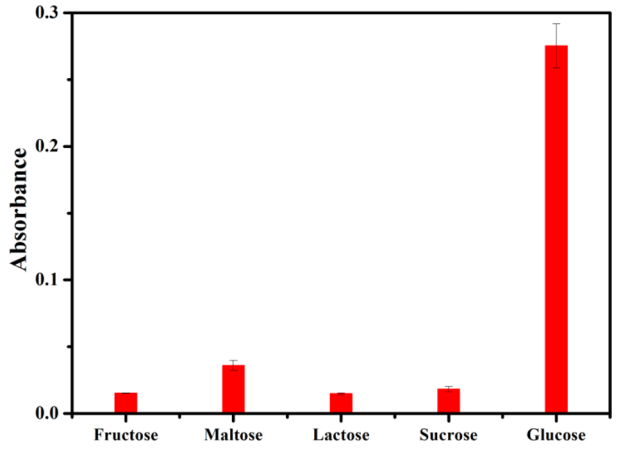

Figure 4. Selective determination in the presence of different interferents. The final concentrations of the relative species were as follows: fructose, 25 mM; maltose, 25 mM; sucrose, 25 mM; lactose, 25 mM; glucose, 5 mM. The error bars represent the standard deviation of three measurements.

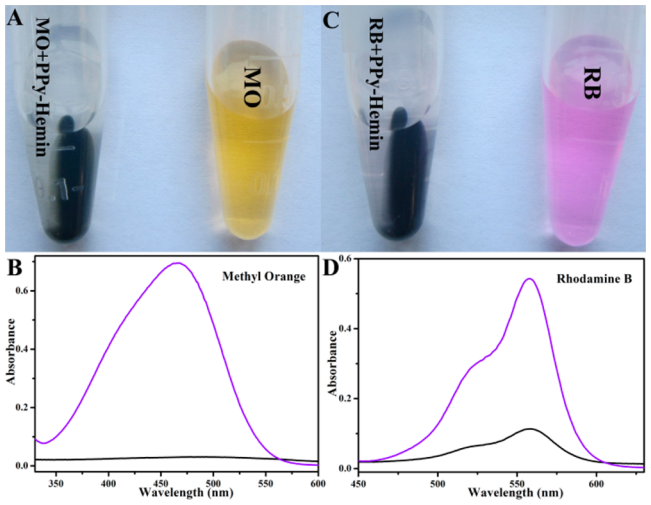

Figure 5. The removal of methyl orange (A, B) and rhodamine B (C, D) before and after adding PPy/hemin.

producing a blue color, but also catalyzed OPDA to give an orange color, verifying its peroxidase-mimic property.

3.3. Glucose Determination. Glucose detection is a common but necessary analysis in clinic and laboratory. Generally, H_2O_2 is a product of enzymatic reactions by GOD with glucose in the presence of oxygen. Therefore, a simple colorimetric method was developed to detect glucose by integrating GOD and PPy/hemin nanocomposite. In the presence of glucose, the enzymatic reaction's product can be catalyzed by PPy/hemin to form hydroxyl radical. A chromogenic reaction then occurred between hydroxyl radical and TMB, obtaining a remarkable colorimetric signal. As a result, glucose can be indirectly detected by monitoring the color variation. Compared to the traditional protein-based peroxidases, such as horseradish peroxidase, the PPy/hemin nanocomposite is cost-effective and highly stable.

In order to achieve the optimum assay performance, it is necessary to optimize the dose of PPy/hemin. The catalytic reaction was kept at 37 °C for 20 min in the presence of target by adding different volumes of PPy/hemin to the system. The experimental results are shown in Figure S3 (Supporting Information). As the volumes increased, the absorbance was intensified rapidly, implying more TMB molecules were catalyzed. The maximum absorbance value was observed when the volumes increased to 10 μL. However, a further increase in volumes could not augment the absorbance. Therefore, we adopted 10 μL as the optimal dosage for subsequent analysis.

Under the optimal conditions, the sensitivity of the described strategy towards target molecule was investigated by adding a series of different concentrations of glucose to the catalytic system. Figure 3 shows the absorbance changes in response to varying concentrations of glucose ranging from 0 to 10.00 mM. As the glucose concentration increased, an obvious absorbance augment was observed, demonstrating a concentration dependent response. Figure 3B (inset) shows the calibration curve for quantitative analysis of glucose. The absorbance value was linearly dependent on glucose concentration in the range from 0.05 to 8.00 mM. The calibration equation was $A = 0.16C_{Glucose}$

dx.doi.org/10.1021/am404539j | ACS Appl. Mater. Interfaces 2014, 6, 500−506

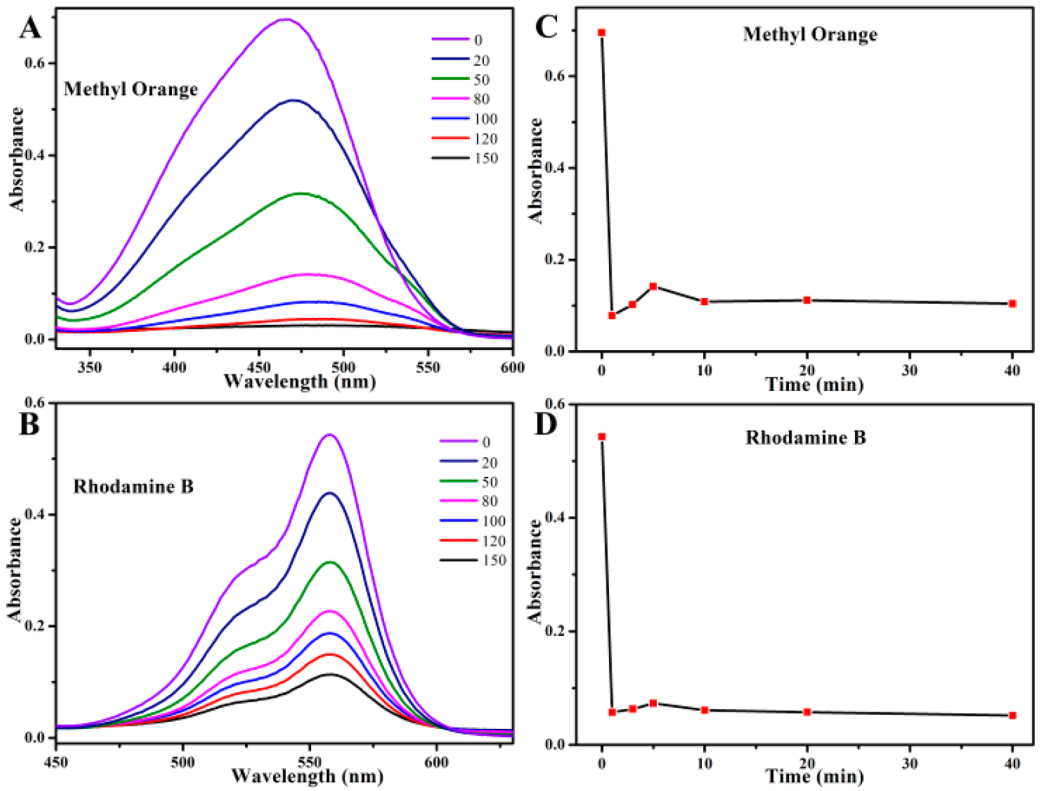

Figure 6. Adsorption isotherm of methyl orange (A) and rhodamine B (B) at different volumes of PPy/hemin (1 mg/mL) (temperature 25 °C, pH 7.0). Kinetic adsorption data for methyl orange (C) and rhodamine B (D). The initial concentration of the dye solutions was 10 mg/L, and PPy/hemin (1 mg/mL) was 150 μL.

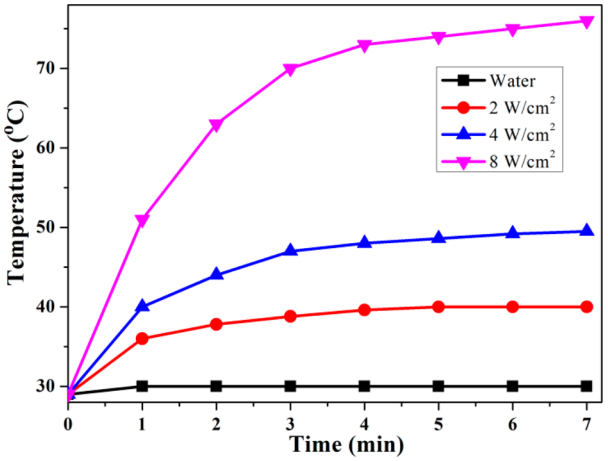

Figure 7. The photothermal effects of PPy/hemin with a 808 nm laser at different power densities.

+ 2.73 × 10^{-2} and A = 7.19 × $10^{-2}C_{Glucose}$ + 0.29 (A is the absorbance at 452 nm, and C is the concentration of glucose), and the calibration coefficient is R = 0.997 and 0.999, respectively. The detection limit was experimentally determined to be 50 μM (Figure S4, Supporting Information). This value was superior to those of many reported homogeneous assay techniques.[51−53] It is worth noting that the unique property of PPy/hemin makes it suitable for the application in a glucose biosensor. On the one hand, excellent biocompatibility of PPy/hemin could provide a friendly environment to retain GOD's bioactivity, enhancing the catalytic efficiency of GOD. On the other hand, the high surface area of PPy/hemin provides a significant increase for GOD loading on the material surface, which allows GOD's catalysate to easily diffuse into the interior of the particle and improve the catalytic efficiency, as well as the detection sensitivity. The experimental results demonstrated that the present method could serve as a sensitive colorimetric sensing platform for glucose detection.

In this assay, the selectivity of the proposed strategy was evaluated by using glucose analogues fructose, maltose, sucrose, and lactose as interfering species. As can be seen in Figure 4, although the concentrations of the interfering molecules outweigh that of the target by 5 times, a remarkable signal increase was only obtained in the presence of a target molecule. Upon addition of interferents mentioned above, no obvious absorbance signal changes were observed compared with the target. The results demonstrated that the glucose biosensor possessed a quite good anti-interference ability for possible practical applications.

3.4. Adsorption Property. Most dyes are toxic, carcinogenic, and mutagenic. However, a large number of dyes untreated are discharged in wastewater every year, resulting in adverse effects on human and animal health. Therefore, it is very urgent to develop new materials to remove the dye pollutants from waste water.[54] We then investigated the adsorption ability of PPy/hemin using MO and RB as model pollutants. Figure 5 shows the experimental results for the sorption of MO and RB onto PPy/hemin. A dramatic absorbance drop was observed after adding PPy/hemin to the dye solutions, illustrating superb adsorption ability to the dye molecules. It should be noted that the relatively high surface area and mesoporous structure of the as-prepared materials endowed itself good adsorption properties for potential

dx.doi.org/10.1021/am404539j | ACS Appl. Mater. Interfaces 2014, 6, 500−506

applications in dye removal. Moreover, the dye removal could be easily visualized by the color variation of the dye solutions (shown in the Figure 5A and C).

To obtain an optimal sorption capacity, the relation between the adsorbent dosage and the removal of dye was studied by varying the adsorbent quantity while keeping the initial dye concentration constant. As indicated in Figure 6A, the characteristic UV−vis absorption of MO at 466 nm (RB at 558 nm, Figure 6B) decreased upon increasing the volume of PPy/hemin aqueous solution. When the volume of PPy/hemin was increased to 150 μL, over 94 % of MO could be removed within 5 min at room temperature. Also, the adsorption efficiency tended to level off after more dosage of the PPy/hemin was added. As for RB, the removal efficiency reached 90 % after 150 μL of PPy/hemin was added. We also investigated the adsorption kinetics during the adsorption process. Parts C and D of Figure 6 show the data for adsorption of dye solutions by PPy/hemin at different time intervals. Over 90% adsorption occurred within the first 1 min for MO and RB, respectively, suggesting that PPy/hemin had ultrafast adsorption kinetics toward dye solutions. The experimental results demonstrated clearly that the PPy/hemin was an excellent adsorbent for dye removal.

3.5. Photothermal Effect. As one of the photothermal therapy materials, NIR-absorbing nanomaterials have received numerous considerations due to their minimal absorbance and maximum penetration for tissues and organ tissues in this wavelength regime.[55−66] Interestingly, the synthesized PPy/hemin naoncomposite also showed a strong and broad absorption in the NIR region, implying a promising application as a photothermal agent. To reveal the potential application of the nanocomposite as the photothermal agent, the effect of laser activated temperature increase of the PPy/hemin solution was evaluated under different laser power densities and irradiation times. As can be seen in Figure 7, an obvious temperature increase was observed at first and then remained constant after 7 min when PPy/hemin solution was irradiated at 808 nm with different power densities. Accordingly, the final temperature of the solution increased with enhancing laser power density. However, the solution's temperature without PPy/hemin remained unchanged under irradiation at 808 nm (8 $W \cdot cm^{-2}$). Additionally, the nanocomposite exhibited great photostability even after laser exposure for a long time (data not shown). These results indicated that the nanocomposite was efficiently responsive to the NIR light, and the excellent photothermal conversion efficiency and photostability make it an encouraging agent for photothermal cancer treatment.

4. CONCLUSION

In summary, we presented a simple one-pot template method for producing a PPy/hemin nanocomposite by using cost-effective precursors. Benefiting from the combined advantages of PPy and hemin, the nanocomposite exhibited intrinsic peroxidase-like activity and provided a colorimetric assay for glucose. The colorimetric method displayed a good response toward glucose detection with a linear range from 0.05 to 8.00 mM. Due to their easy preparation, robustness, and stability in rough conditions, the nanocomposite can rival natural enzymes and show great potential applications in a variety of simple, robust, cost-effective, and easy-to-make biosensors. The nanocomposite also suggested effective adsorbents for removal of dye pollutants from aqueous solution in a short time, and thus can be used as a new platform for dye decontamination. Moreover, the nanomaterials showed a strong and broad absorption in the NIR region, implying a promising application as the photothermal agent. It should be noted that the unique nature of PPy/hemin nanocomposite makes it very promising for the fabrication of inexpensive, high-performance bioelectronic devices in the future.

■ ASSOCIATED CONTENT

Ⓢ Supporting Information

Photographs of the control experiment and oxidation of *O*-phenylenediamine, graph plots showing the effects of the volume of PPy/hemin, and detection limit of glucose which is experimentally obtained. This material is available free of charge via the Internet at http://pubs.acs.org.

■ AUTHOR INFORMATION

Corresponding Author

*E-mail: dongsj@ciac.ac.cn.

Notes

The authors declare no competing financial interest.

■ ACKNOWLEDGMENTS

This work was supported by National Natural Science Foundation of China (Nos. 20935003, 21075116) and the 973 Project (Nos. 2010CB933603, 2011CB911002).

■ REFERENCES

(1) Miomandre, F.; Chandezon, F.; Lama, B.; Besnardiere, J.; Routier, M.; Brosseau, A.; Audebert, P. *J. Nanopart. Res.* **2011**, *13*, 879−886.
(2) Zhang, H.; Li, L.; Moller, M.; Zhu, X.; Rueda, J. J. H.; Rosenthal, M.; Ivanov, D. A. *Adv. Mater.* **2013**, *25*, 3543−3548.
(3) Tran, H. V.; Piro, B.; Reisberg, S.; Tran, L. D.; Duc, H. T.; Pham, M. C. *Biosens. Bioelectron.* **2013**, *49*, 164−169.
(4) Sun, B.; Long, Y. Z.; Liu, S. L.; Huang, Y. Y.; Ma, J.; Zhang, H. D.; Shen, G.; Xu, S. *Nanoscale* **2013**, *5*, 7041−7045.
(5) Sosnowska, M.; Pieta, P.; Sharma, P. S.; Chitta, R.; Kc, C. B.; Bandi, V.; D'Souza, F.; Kutner, W. *Anal. Chem.* **2013**, *85*, 7454−7461.
(6) Qiao, J.; Zhang, J.; Zhang, J. *J. Power Sources* **2013**, *237*, 1−4.
(7) Liu, Z.; Liu, Y.; Poyraz, S.; Zhang, X. *Chem. Commun.* **2011**, *47*, 4421−4423.
(8) Safarnavadeh, V.; Zare, K.; Fakhari, A. R. *Biosens. Bioelectron.* **2013**, *49*, 159−163.
(9) Liu, B.; Wang, X. L.; Lian, H. T.; Sun, X. Y. *Anal. Biochem.* **2013**, *440*, 220−226.
(10) Deng, F.; Min, L.; Luo, X.; Wu, S.; Luo, S. *Nanoscale* **2013**, *5*, 8703−8710.
(11) Bahloul, A.; Nessark, B.; Briot, E.; Groult, H.; Mauger, A.; Zaghib, K.; Julien, C. M. *J. Power Sources* **2013**, *240*, 267−272.
(12) Lou, B.; Chen, C.; Zhou, Z.; Zhang, L.; Wang, E.; Dong, S. *Talanta* **2013**, *105*, 40−45.
(13) Zhu, C.; Zhai, J.; Wen, D.; Dong, S. *J. Mater. Chem.* **2012**, *22*, 6300−6306.
(14) Girotto, E. M.; De Paoli, M. A. *Adv. Mater.* **1998**, *10*, 790−793.
(15) Lascelles, S. F.; McCarthy, G. P.; Butterworth, M. D.; Armes, S. P. *Colloid Polym. Sci.* **1998**, *276*, 893−902.
(16) Travascio, P.; Li, Y. F.; Sen, D. *Chem. Biol.* **1998**, *5*, 505−517.
(17) Tang, D.; Yuan, R.; Chal, Y. *Anal. Chem.* **2008**, *80*, 1582−1588.
(18) Tang, D.; Ren, J. *Anal. Chem.* **2008**, *80*, 8064−8070.
(19) Song, Z.; Yuan, R.; Chai, Y.; Zhuo, Y.; Jiang, W.; Su, H.; Che, X.; Li, J. *Chem. Commun.* **2010**, *46*, 6750−6752.
(20) Gao, Z.; Xu, M.; Hou, L.; Chen, G.; Tang, D. *Anal. Chim. Acta* **2013**, *776*, 79−86.
(21) Walsh, M. T.; Connell, K.; Glynn, S. F.; Costello, R. W.; Asthma Res, G. *Am. J. Respir. Crit. Care Med.* **2009**, *179*, A3700.

(22) Liu, J. R.; Hinkhouse, M. M.; Sun, W. Q.; Weydert, C. J.; Ritchie, J. M.; Oberley, L. W.; Cullen, J. J. *Hum. Gene Ther.* **2004**, *15*, 239−250.
(23) Banning, A.; Kipp, A.; Schmitmeier, S.; Loewinger, M.; Florian, S.; Krehl, S.; Thalmann, S.; Thierbach, R.; Steinberg, P.; Brigelius-Flohe, R. *Cancer Res.* **2008**, *68*, 9746−9753.
(24) Walsh, M. T.; Connell, K.; Sheahan, A. M.; Gleich, G. J.; Costello, R. W. *Am. J. Respir. Cell Mol. Biol.* **2011**, *45*, 946−952.
(25) Zhai, R.; Zhang, B.; Wan, Y.; Li, C.; Wang, J.; Liu, J. *Chem. Eng. J.* **2013**, *214*, 304−309.
(26) Niu, J.; Xu, J.; Dai, Y.; Xu, J.; Guo, H.; Sun, K.; Liu, R. *J. Hazard. Mater.* **2013**, *246*, 119−125.
(27) Kim, H. J.; Suma, Y.; Lee, S. H.; Kim, J.-A.; Kim, H. S. *J. Mol. Catal. B: Enzym.* **2012**, *83*, 8−15.
(28) Xie, Q.; Zhao, Y.; Chen, X.; Liu, H.; Evans, D. G.; Yang, W. *Biomaterials* **2011**, *32*, 6588−6594.
(29) Pusch, J. M. E.; Brondani, D.; Luza, L.; Dupont, J.; Vieira, I. C. *Analyst* **2013**, *138*, 4898−4906.
(30) Nieh, C. H.; Kitazumi, Y.; Shirai, O.; Kano, K. *Biosens. Bioelectron.* **2013**, *47*, 350−355.
(31) Ghourchian, H.; Hong, J.; Hamidi, F. *Clin. Biochem.* **2011**, *44*, S96−S96.
(32) Orozco, J.; Garcia-Gradilla, V.; D'Agostino, M.; Gao, W.; Cortes, A.; Wang, J. *ACS Nano* **2013**, *7*, 818−824.
(33) Lin, Y.; Zhao, A.; Tao, Y.; Ren, J.; Qu, X. *J. Am. Chem. Soc.* **2013**, *135*, 4207−4210.
(34) Haugner, J. C., III; Seelig, B. *Chem. Commun.* **2013**, *49*, 7322−7324.
(35) Dong, Z.; Luo, Q.; Liu, J. *Chem. Soc. Rev.* **2012**, *41*, 7890−7908.
(36) Miao, L.; Zhang, K.; Qiao, C.; Jin, X.; Zheng, C.; Yang, B.; Sun, H. *Nanomedicine: Nanotechnol. Biol. Med.* **2013**, *9*, 141−150.
(37) Wang, Q.; Yang, Z.; Zhang, X.; Xiao, X.; Chang, C. K.; Xu, B. *Angew. Chem., Int. Ed.* **2007**, *46*, 4285−4289.
(38) Gharibi, H.; Moosavi-Movahedi, Z.; Javadian, S.; Nazari, K.; Moosavi-Movahedi, A. A. *J. Phys. Chem. B* **2011**, *115*, 4671−4679.
(39) Ge, P. Y.; Zhao, W.; Du, Y.; Xu, J. J.; Chen, H. Y. *Biosens. Bioelectron.* **2009**, *24*, 2002−2007.
(40) Fruk, L.; Niemeyer, C. M. *Angew. Chem., Int. Ed.* **2005**, *44*, 2603−2606.
(41) Guo, Y.; Deng, L.; Li, J.; Guo, S.; Wang, E.; Dong, S. *ACS Nano* **2011**, *5*, 1282−1290.
(42) Zhang, L.; Zhu, J.; Li, T.; Wang, E. *Anal. Chem.* **2011**, *83*, 8871−8876.
(43) Zhu, J.; Li, T.; Zhang, L.; Dong, S.; Wang, E. *Biomaterials* **2011**, *32*, 7318−7324.
(44) Tian, B.; Zerbi, G. *J. Chem. Phys.* **1990**, *92*, 3886−3891.
(45) Maeda, S.; Corradi, R.; Armes, S. P. *Macromolecules* **1995**, *28*, 2905−2911.
(46) Ravichandran, S.; Nagarajan, S.; Kokil, A.; Ponrathnam, T.; Bouldin, R. M.; Bruno, F. F.; Samuelson, L.; Kumar, J.; Nagarajan, R. *Langmuir* **2012**, *28*, 13380−13386.
(47) Jones, P.; Mantle, D.; Davies, D. M.; Kelly, H. C. *Biochemistry* **1977**, *16*, 3974−3978.
(48) Portsmou, D.; Beal, E. A. *Eur. J. Biochem.* **1971**, *19*, 479−487.
(49) Janchen, M.; Scheller, F.; Prumke, H. J.; Mohr, P. *Acta Biol. Med. Ger.* **1975**, *34*, 319−324.
(50) Balla, G.; Jacob, H. S.; Eaton, J. W.; Belcher, J. D.; Vercellotti, G. M. *Arterioscler., Thromb., Vasc. Biol.* **1991**, *11*, 1700−1711.
(51) Jin, L.; Shang, L.; Guo, S.; Fang, Y.; Wen, D.; Wang, L.; Yin, J.; Dong, S. *Biosens. Bioelectron.* **2011**, *26*, 1965−1969.
(52) Shen, X. W.; Huang, C. Z.; Li, Y. F. *Talanta* **2007**, *72*, 1432−1437.
(53) Amarie, D.; Alileche, A.; Dragnea, B.; Glazier, J. A. *Anal. Chem.* **2010**, *82*, 343−352.
(54) Sun, H.; Cao, L.; Lu, L. *Nano Res.* **2011**, *4*, 550−562.
(55) Zhou, W.; Liu, X.; Ji, J. *J. Nanopart. Res.* **2012**, *14*, 1128−1143.
(56) Yang, K.; Xu, H.; Cheng, L.; Sun, C.; Wang, J.; Liu, Z. *Adv. Mater.* **2012**, *24*, 5586−5592.
(57) Li, N.; Yu, Z.; Pan, W.; Han, Y.; Zhang, T.; Tang, B. *Adv. Funct. Mater.* **2013**, *23*, 2255−2262.
(58) Weissleder, R. *Nat. Biotechnol.* **2001**, *19*, 316−317.
(59) von Maltzahn, G.; Park, J. H.; Agrawal, A.; Bandaru, N. K.; Das, S. K.; Sailor, M. J.; Bhatia, S. N. *Cancer Res.* **2009**, *69*, 3892−3900.
(60) Kennedy, L. C.; Bickford, L. R.; Lewinski, N. A.; Coughlin, A. J.; Hu, Y.; Day, E. S.; West, J. L.; Drezek, R. A. *Small* **2011**, *7*, 169−183.
(61) Skrabalak, S. E.; Au, L.; Lu, X.; Li, X.; Xia, Y. *Nanomedicine (London, U.K.)* **2007**, *2*, 657−668.
(62) Giljohann, D. A.; Seferos, D. S.; Daniel, W. L.; Massich, M. D.; Patel, P. C.; Mirkin, C. A. *Angew. Chem., Int. Ed.* **2010**, *49*, 3280−3294.
(63) Alkilany, A. M.; Thompson, L. B.; Boulos, S. P.; Sisco, P. N.; Murphy, C. J. *Adv. Drug Delivery Rev.* **2012**, *64*, 190−199.
(64) Loo, C.; Lowery, A.; Halas, N. J.; West, J.; Drezek, R. *Nano Lett.* **2005**, *5*, 709−711.
(65) Jain, P. K.; Huang, X.; EI-Sayed, I. H.; EI-Sayed, M. A. *Acc. Chem. Res.* **2008**, *41*, 1578−1586.
(66) O'Neal, D. P.; Hirsch, L. R.; Halas, N. J.; Payne, J. D.; West, J. L. *Cancer Lett.* **2004**, *209*, 171−176.